DOI: 10.1002/ejic.201100660

A New Metal Carboxylate Framework Based on Porphyrin with Extended π-Conjugation

Satoshi Matsunaga,*[a] Nanako Endo,[a] and Wasuke Mori*[a]

Keywords: Microporous materials / Zinc / Metal–organic frameworks / Porphyrinoids / Carboxylate ligands

We have designed a new tetracarboxylporphyrin building block, ZnTCPEP-H_4, and used it in the construction of a novel porphyrin-based metal carboxylate framework, $[Zn_4(\mu_3\text{-}OH)_2(H_2O)_2(ZnTCPEP\text{-}H)_2(DABCO)]\cdot 2DMF\cdot 10.5H_2O$ (Zn_4·ZnTCPEP·DABCO). The framework forms a 3D network linked by tetranuclear Zn cluster nodes $\{Zn_4(\mu_3\text{-}OH)_2(H_2O)_2\}$, ZnTCPEP-$H_4$, and DABCO. The ZnTCPEP-H_4 building block exhibits extended π-conjugation from the porphyrin core to the terminal carboxyl groups via ethynyl linkers attached to the porphyrin core. The Zn_4·ZnTCPEP·DABCO framework gives rise to a 3D porous structure containing open channels with cross sections of approximately 10 × 10 and 7 × 7 Å. It has a BET surface area of 461 m^2/g and a Langmuir surface area of 581 m^2/g. A hydrogen adsorption capacity of 0.86 wt.-% was determined for Zn_4·ZnTCPEP·DABCO at 77 K and 0.1 MPa.

Introduction

Porous metal–organic frameworks (MOFs) have attracted much attention because of their potential applications in various fields, including gas storage,[1,2d–2f] gas separation,[3] ion exchange,[4] and catalysis.[2,5] In order to further functionalize MOFs, it is important to incorporate functional ligands as the MOF building blocks. The use of functional building blocks provides a unique opportunity to add desirable ligand-intrinsic properties to the frameworks. Many studies have been reported, in which functional building blocks, such as metallosalens,[6] metalloporphyrins,[7] carboranes,[8] and polyoxometalates,[9] were used. Metalloporphyrins in particular can be found throughout nature and have unique catalytic, electronic, and optical properties.[10] The physical and chemical properties of metalloporphyrins can be controlled by proper functionalization of the porphyrin core through standard modifications. Using metalloporphyrins as MOF building blocks offers the potential to tailor the photochemical and redox properties of the frameworks. Additionally, by incorporating accessible metal sites (AMSs) into MOFs, their catalytic activity and gas adsorption capacity can be enhanced. Metalloporphyrins are also one of the best building blocks for incorporation of AMSs into MOFs.

We have studied porphyrin-based microporous MOFs and a multicarboxylporphyrin derivative in particular, tetrakis(4-carboxyphenyl)porphyrin (TCPP), as a potential building block.[2] In 2003, we synthesized a rhodium carboxylate microporous MOF containing H_2TCPP, $[Rh_2(H_2TCPP)]_n$, and reported on its gas adsorption ability and catalytic activity for the hydrogenation of ethylene and propylene.[2a] In 2005, we also reported that rhodium carboxylate microporous MOFs incorporating various metallo-TCPPs, that is, $[Rh_2(MTCPP)]$ (M = H_2, Cu^{2+}, Ni^{2+}, Pd^{2+}), showed high turnover frequencies for the hydrogenation of olefins, and the catalytic activities depended on the type of metal center coordinated to the porphyrin ring, which means that the metallo-TCPPs exhibit a bimetallic effect.[2b] Recently, Choe and co-workers reported on the crystal structure and hydrogen adsorption capacity of a similar compound, $[Zn_2(ZnTCPP)]$, in which Zn^{2+} was used as the node metal.[7h] Furthermore, many other supramolecular structures constructed by self-assembly of TCPP derivatives have been reported; especially well known are the significant works by Goldberg and co-workers.[11] Most recently, Farha and co-workers reported on robust porphyrinic materials (RPMs).[7k]

However, the multicarboxylporphyrin derivatives that have been used as MOF building blocks are limited to *meso*-aryl-substituted porphyrins. In *meso*-aryl-substituted porphyrins, the aryl groups are twisted out of the porphyrin plane due to steric hindrance between protons at the β position of the porphyrin core and protons at the *ortho* positions of the aryl groups. Therefore, the porphyrin plane is not coplanar with the carboxyl planes, which results in the interruption of the π-conjugation (Figure 1a). To solve this problem, we have designed a novel porphyrin derivative, TCPEP (Figure 1b), in which the four carboxyphenyl groups are attached to the porphyrin core via ethynyl linkers. The carboxyl planes of TCPEP are almost coplanar with the porphyrin plane due to a lack of steric hindrance. By using TCPEP as MOF building blocks, it is possible to

---

[a] Department of Chemistry, Faculty of Science, Kanagawa University, Hiratsuka,
Kanagawa 259–1293, Japan
E-mail: matsunaga@kanagawa-u.ac.jp

Supporting information for this article is available on the WWW under http://dx.doi.org/10.1002/ejic.201100660.

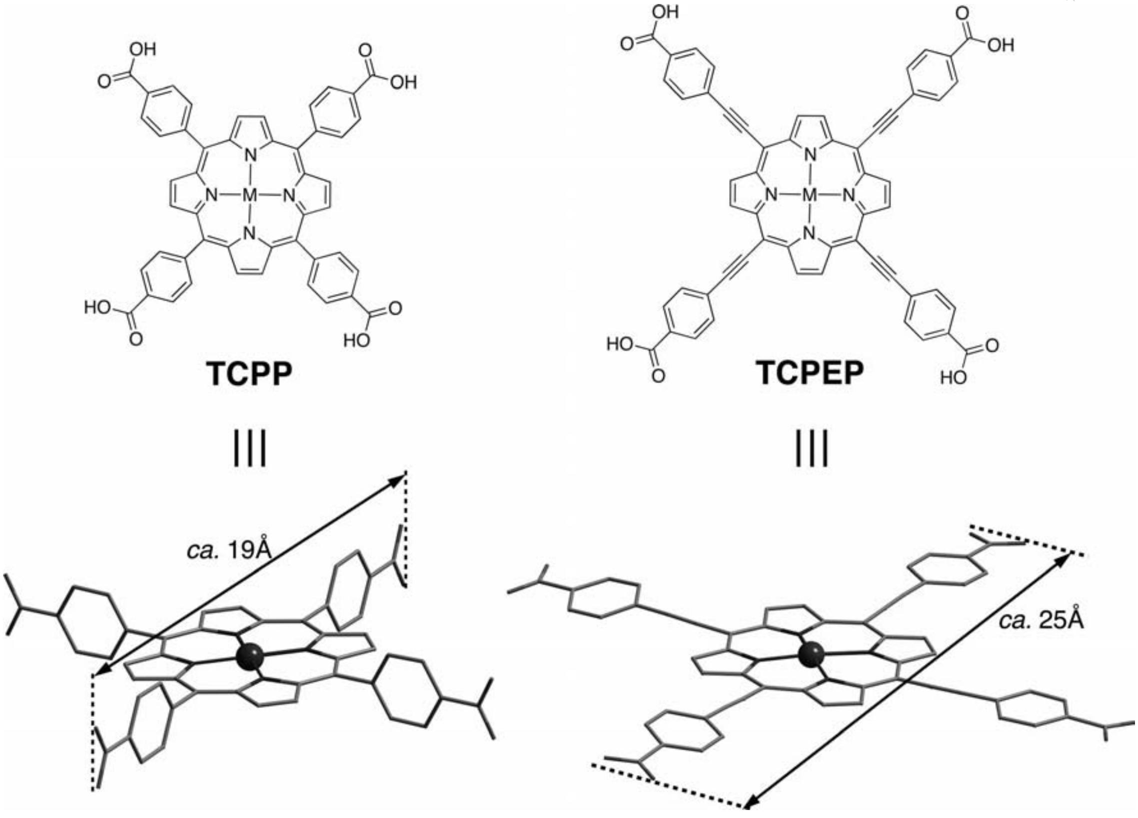

Figure 1. TCPP and the designed TCPEP porphyrin ligand.

construct new structural MOFs with properties derived from a large π-conjugated system. In this paper we report on the construction of novel porphyrin-based metal carboxylate frameworks $[Zn_4(\mu_3\text{-}OH)_2(H_2O)_2(ZnTCPEP\text{-}H)_2(DABCO)]\cdot 2DMF\cdot 10.5H_2O$ ($Zn_4\cdot$ZnTCPEP·DABCO) with 3D network topology synthesized by using a ZnTCPEP linker and discuss their detailed synthesis, crystal structure, and gas adsorption properties.

Results and Discussion

Synthesis

The syntheses of the ZnTCPEP-H_4 building blocks and $Zn_4\cdot$ZnTCPEP·DABCO are summarized in Scheme 1. Compounds **2**–**4** were prepared according to literature procedures.[12] Lithiation of TIPS-acetylene (**1**) followed by acylation with 4-formylmorpholine afforded TIPS-propiolic aldehyde (**2**). The tetra-TIPS-ethynyl-substituted zinc porphyrin **4** was prepared by condensation of pyrrole with **2** and subsequent heating of the resultant porphyrin **3** with $Zn(OAc)_2\cdot 2H_2O$ in $CHCl_3$. Deprotection of the tetra-TIPS-ethynyl-substituted porphyrin **4** with tetrabutylammonium fluoride (TBAF) yielded the deprotected ethynylporphyrin, which was then coupled to methyl-4-iodobenzene under copper-free Sonogashira coupling conditions[13] to give the tetraester porphyrin ZnTCPEP-Me_4. Basic hydrolysis of the tetraester ZnTCPEP-Me_4 gave the tetracarboxylic acid building block ZnTCPEP-H_4. Subsequent reaction of ZnTCPEP-H_4 with $Zn(NO_3)_2\cdot 6H_2O$ and DABCO (1,4-diazabicyclo[2.2.2]octane) in DMF/EtOH at 80 °C for 24 h afforded dark green single crystals of $Zn_4\cdot$ZnTCPEP·DABCO. According to elemental and thermogravimetric/differential thermal analyses (TG/DTA), the single crystals of $Zn_4\cdot$ZnTCPEP·DABCO contain two DMF molecules, 10.5 water molecules, and two coordinating water molecules and have the formula $[Zn_4(\mu_3\text{-}OH)_2(H_2O)_2(ZnTCPEP\text{-}H)_2(DABCO)]\cdot 2DMF\cdot 10.5H_2O$ (Figure S1).

Absorption Spectra of the ZnTCPEP-H_4 Building Block

The UV/Vis absorption spectra of the ZnTCPEP-H_4 building block and ZnTCPP as a reference compound are shown in Figure 2. The absorption spectrum of ZnTCPEP-H_4 in DMF shows a Soret band at 485 nm, together with smaller Q-bands at 633 and 687 nm. All bands are red-shifted relative to ZnTCPP (Soret band: 428 nm, Q-bands: 560, 600 nm). The large redshifts of both the Soret band and the Q-bands indicate a decreased energy gap between the HOMO and LUMO orbitals, a consequence of the expanded π-conjugation. In the *meso*-aryl-substituted porphyrins, the aryl groups are twisted out of the porphyrin plane due to steric hindrance between the protons at the β position of the porphyrin core and protons at the *ortho* positions of the aryl groups, resulting in interruption of the π-conjugation. In contrast, the carboxyphenyl plane of ZnTCPEP-H_4 is coplanar with the porphyrin plane, because the porphyrin core and aryl groups at the *meso*-posi-

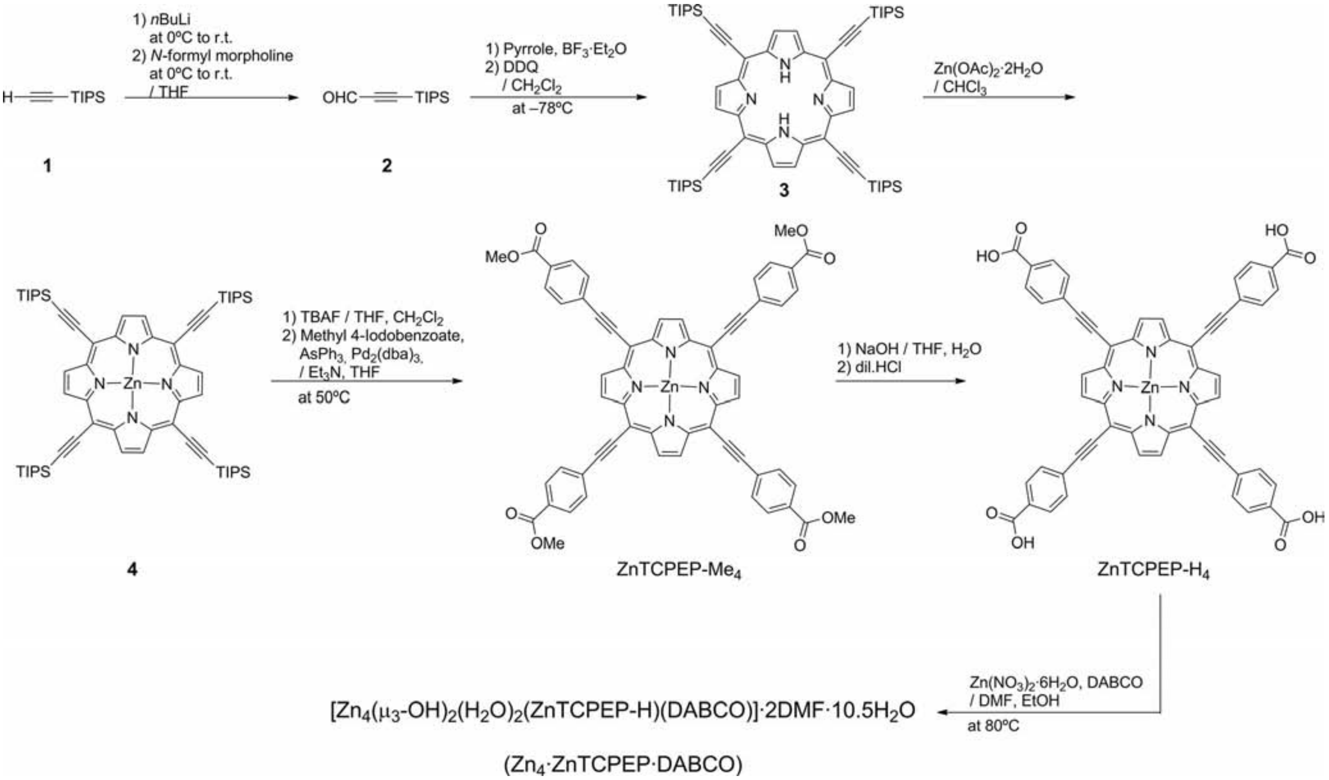

Scheme 1. Syntheses of the ZnTCPEP-H_4 building block and Zn_4·ZnTCPEP·DABCO.

tion are linked via an ethynyl spacer. Therefore, ZnTCPEP-H_4 exhibits extended π-conjugation from the porphyrin core to the terminal carboxyl groups. The large absorption in the visible region indicates that ZnTCPEP-H_4 can be a building block for visible-light-sensitive functionalized MOFs.

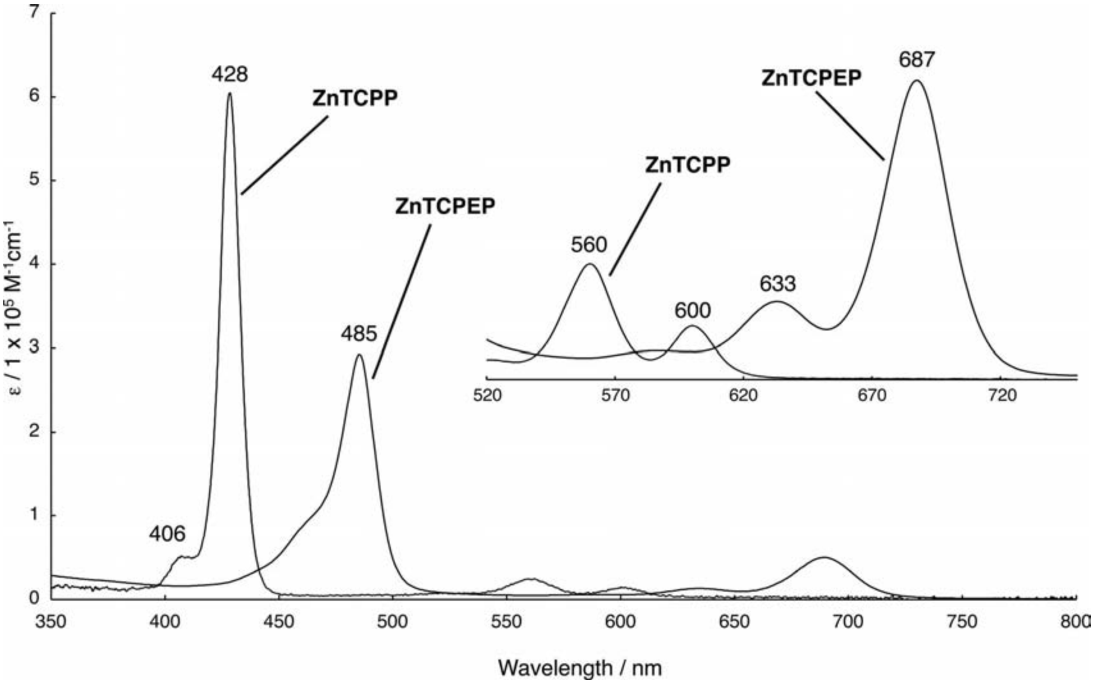

Figure 2. UV/VIS absorption spectra of ZnTCPEP-H_4 and ZnTCPP in DMF. Inset shows enlarged view.

Structural Characterization of Zn_4·ZnTCPEP·DABCO

Single-crystal X-ray analysis revealed that Zn_4·ZnTCPEP·DABCO crystallizes in the orthorhombic *Ccca* space group. The ZnTCPEP-H_4 units are linked by a tetranuclear zinc cluster, that is, $\{Zn_4(\mu_3\text{-}OH)(H_2O)_2\}$, and DABCO units, resulting in the formation of a 3D framework. In the cluster unit, two crystallographically independent Zn atoms exist: (i) Zn(2) is tetrahedrally coordinated, binding to two O atoms from two carboxylate groups, one O atom from a μ_3-OH, and one nitrogen atom of a DABCO unit connected to Zn(1) of ZnTCPEP; (ii) Zn(3) is octahedrally coordinated, binding to three O atoms from two carboxylate groups, two O atoms from two μ_3-OH, and one O atom from a H_2O (Figure 3a). The bond valence sums (BVSs),[14] calculated from the observed bond lengths, are 1.365 for the O(9) atom and 0.351 for the O(10) atom, which reasonably correspond to those of OH^- and H_2O, respectively. A tetranuclear zinc cluster node similar to that observed in Zn_4·ZnTCPEP·DABCO has been reported for $Zn_4(OH)_2(H_2O)_2(py)_2(TCBPB)_2$·3DMF·py·3$H_2O$ (TCBPB = 1,3,5-tris[4′-carboxy(1,1′-biphenyl4-yl)]benzene, py = pyridine).[15] In the present case, X-ray analysis revealed a high coplanarity of the porphyrin core, the phenyl groups, and the carboxylate groups within the ZnTCPEP moiety (average torsion angle between the phenyl ring and the porphyrin core: 5.98° in ZnTCPEP compared to 80.14° in ZnTCPP[7h]). Three of the four carboxylate groups of ZnTCPEP are coordinated to the Zn_4 cluster, while the remaining group is present as a free carboxylic acid (Figure 3b). Each of the three coordinating carboxylate groups shows different coordination modes: two oxygen atoms [O(1) and O(2)] linking two zinc atoms [Zn(2) and Zn(3)], two oxygen atoms [O(3) and O(4)] coordinating one zinc atom [Zn(3)], and one oxygen atom [O(7)] coordinating one zinc atom [Zn(2)]. The C–O distances for the noncoordinating carboxylic acid are 1.224 Å [C(47)–O(5)] and 1.340 Å [C(47)–O(6)], in agreement with typical values for carboxylic acids. The noncoordinating carboxyl group forms a hydrogen bond with a hydrated water molecule [O(11)]. The molecular length of the ZnTCPEP unit (ca. 24 Å) is 125% the length of the ZnTCPP unit (ca. 19 Å) due to the insertion of ethynyl spacers. Every ZnTCPEP unit links three $[Zn_4(\mu_3\text{-}OH)_2(H_2O)_2]$ cluster units, and every cluster unit connects eight ZnTCPEP units via the carboxylate groups and DABCO. This results in a 3D framework with open channels along the diagonal line of the *ab* plane and the *c* axis, which have cross sections of approximately 10 × 10 and 7 × 7 Å, respectively (Figure 4). Although the open channels include some DMF and H_2O molecules, it was not possible to locate the guest solvent molecules without taking into consideration the hydrogen bonding between H_2O and a free carboxylic acid, because of their high disorder. Therefore, the *SQUEEZE* routine of *PLATON* was used to remove the diffraction contribution from these solvents to produce a set of solvent-free diffraction intensities.[16] Three-dimensional porphyrin-based paddle-wheel frameworks have previously been reported by Choe et al.[17] These frameworks were assembled by connecting the intersecting 2D porphyrin paddle-wheel grids through a pyridyl-based organic pillar (e.g., 4,4′-bipyridine), which resulted in a 3D pillared-layer coordination polymer. In contrast, the

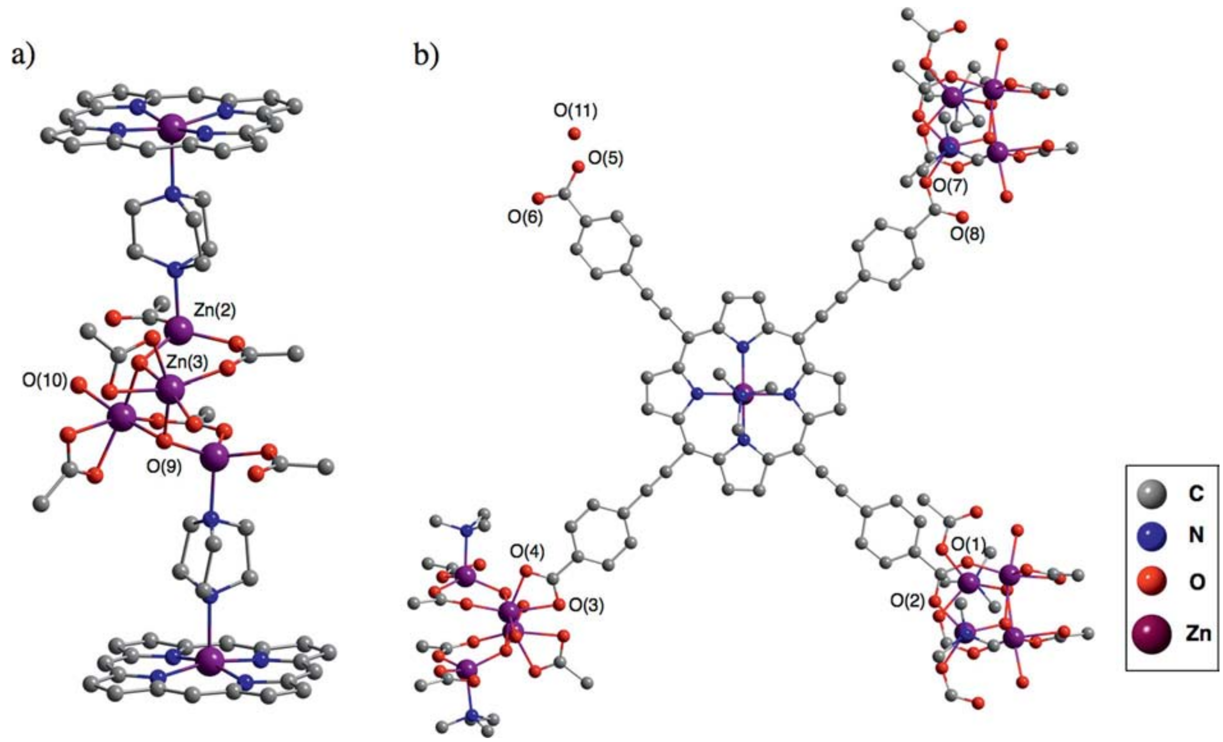

Figure 3. (a) Tetranuclear Zn cluster; (b) ZnTCPEP moiety in Zn_4·ZnTCPEP·DABCO. H atoms are omitted for clarity.

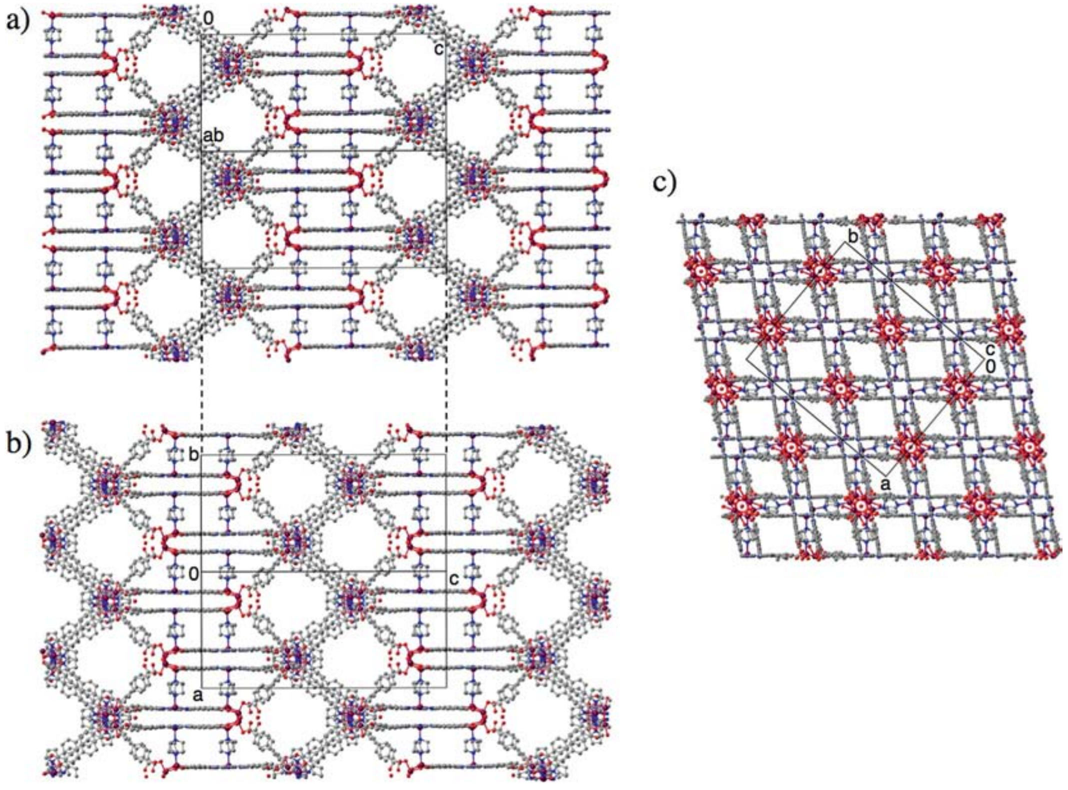

Figure 4. Extended structure of Zn_4·ZnTCPEP·DABCO viewed along (a, b) the diagonal line of the *ab* plane and (c) the crystallographic *c* axis. H atoms are omitted for clarity.

structure of Zn_4·ZnTCPEP·DABCO appears to be a more complicated 3D nonpillared-layer structure. The void volume, calculated from single-crystal structures with *PLATON*/*VOID*, is 56%.[16]

Adsorption Properties

Gas adsorption measurements for N_2 and H_2 at 77 K were performed on Zn_4·ZnTCPEP·DABCO (Figures 5 and 6). The sample was immersed in acetone for several days, to exchange all of the included nonvolatile solvates (DMF, H_2O), and subsequently dried under vacuum at room temp. for 24 h. The nitrogen adsorption isotherm of Zn_4·ZnTCPEP·DABCO (Figure 5) shows type-I behavior, as expected for a microporous compound, indicating the retention of the microporous structure of the framework after removal of the solvent molecules in the channels. The BET surface area is 461 m^2/g, the Langmuir surface area is 581 m^2/g, and the specific micropore volume is 0.2006 cm^3/g. The hydrogen uptake of Zn_4·ZnTCPEP·DABCO was 0.86 wt.-% at 0.1 MPa (Figure 6). A sample evacuated at 100 °C for 24 h showed a lower hydrogen uptake of 0.52 wt.-% under the same conditions. Both the specific surface area and the H_2 uptake of Zn_4·ZnTCPEP·DABCO are lower than the corresponding values of TCPP-based microporous MOFs.[7h] These results may indicate that the desolvation of coordinated H_2O causes partial collapse of the microporous framework structure in Zn_4·ZnTCPEP·DABCO. In fact, gas adsorption measurements on $Zn_4(OH)_2(H_2O)_2(py)_2$-$(TCBPB)_2$·3DMF·py·$3H_2O$, which has a similar tetranuclear zinc cluster node, showed no permanent porosity, possibly, because of a collapse of the framework upon removal of coordinated water and pyridine.[15] The void volume calculated from the N_2 isotherm is 16.5%, which is smaller than that calculated from the single-crystal structures with *PLATON*/*VOID* (56%).[16] The pore diameter distribution of Zn_4·ZnTCPEP·DABCO, calculated accord-

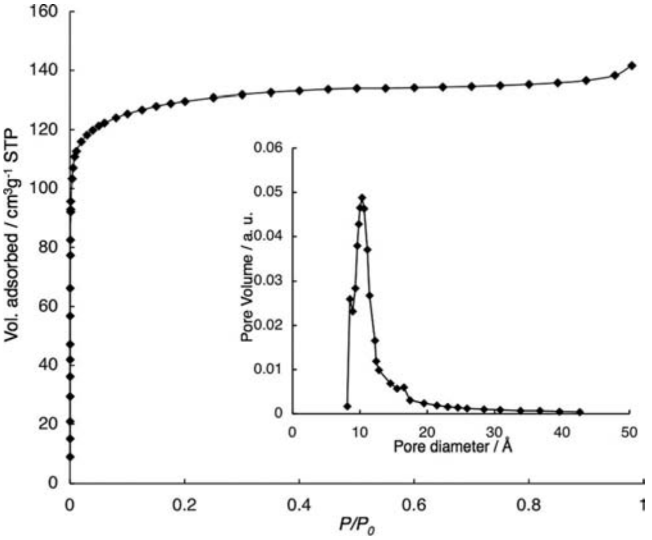

Figure 5. Nitrogen adsorption isotherm at 77 K. Inset: the pore diameter distribution calculated by the Saito–Foley model.

ing to the Saito–Foley model[18] from the adsorption isotherms by using N_2 at 77 K, showed a narrow peak at approximately 10 Å (inset of Figure 5). This pore diameter is consistent with the pore size estimated from the crystal structure and larger than that of the TCPP-based microporous MOFs (ca. 7 Å).

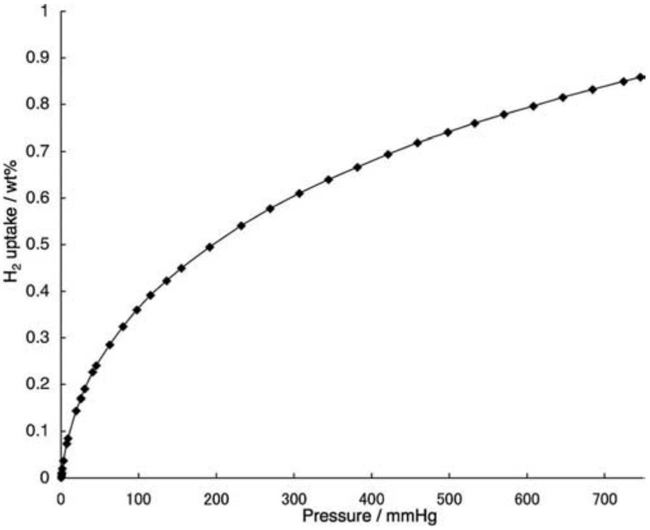

Figure 6. Hydrogen adsorption isotherms at 77 K.

Conclusions

In summary, we have designed a porphyrin-based building block, ZnTCPEP-H_4, in which the porphyrin core, the phenyl groups, and the carboxyl groups are almost coplanar, and used it to synthesize a porphyrin-based MOF, Zn_4·ZnTCPEP·DABCO. This MOF has a 3D porous structure with open channels, which have cross sections of approximately 10 × 10 and 7 × 7 Å. In contrast to the conventional multicarboxylate *meso*-aryl-substituted porphyrins such as ZnTCPP, ZnTCPEP-H_4 exhibits extended π-conjugation from the porphyrin core to the terminal carboxyl groups. Therefore, the Soret and Q-bands are redshifted relative to those of ZnTCPP. The pore diameter of Zn_4·ZnTCPEP·DABCO is also larger than that of the TCPP-based MOFs due to elongation of the building block. The strong absorption in the visible region and large pore diameter of Zn_4·ZnTCPEP·DABCO suggest its use as a visible-light-sensitive functionalized MOF for photocatalysis.

Experimental Section

General Methods: ^{1}H NMR (400 MHz) spectroscopic data were recorded for samples in 5 mm tubes (outer diameter) with a JEOL JNM-EX 400 FTNMR spectrometer and a JEOL EX-400 NMR spectroscopic data-processing system. Elemental analyses were carried out with a Perkin–Elmer 2400 CHNS Elemental Analyzer II (Kanagawa University). Infrared spectra were recorded with a Jasco 4100 FTIR spectrometer by using KBr disks at room temperature. Thermogravimetric (TG) and differential thermal analyses (DTA) were acquired with a Rigaku Thermo Plus 2 series TG/DTA TG 8120 instrument. Adsorption isotherm measurements were performed with an automatic volumetric adsorption apparatus (ASAP2010). The as-synthesized sample was immersed in acetone for several days to exchange all of the included nonvolatile solvates (DMF, H_2O). The adsorbate was placed in a sample tube, which was then evacuated by using the degas function of the analyzer at room temp. for 24 h prior to measurement. The change in the pressure was monitored, and the degree of adsorption was determined by the decrease in pressure at the equilibrium state. The specific surface area was obtained by the Langmuir and Brunauer–Emmett–Teller (BET) methods. The total pore volume was computed from the amount of gas adsorbed at $p/p_0 = 0.200$, and the micropore volume was calculated by using the Saito–Foley model.

X-ray Crystallography: A green block crystal of $[Zn_4(\mu_3\text{-}OH)_2(H_2O)_2(ZnTCPEP\text{-}H)_2(DABCO)_2]$ ($0.08 \times 0.05 \times 0.03$ mm^3) was surrounded by liquid paraffin (Paratone-N) and analyzed at 90 K. Data: orthorhombic, space group *Ccca*; a = 27.5447(18) Å, b = 32.731(2) Å, c = 44.208(3) Å, V = 39857(4) Å^3, Z = 8, $d_{\text{calcd.}}$ = 1.637 g/cm^3; $\mu(\text{Mo-}K_\alpha)$ = 1.824 mm^{-1}. Data collection was performed with a Bruker SMART APEX CCD diffractometer at 90 K in the range of $1.84° < 2\theta < 55.00°$. The intensity data were automatically corrected for Lorentz and polarization effects during integration. The structure was solved by direct methods (*SIR2004*),[19] followed by difference Fourier calculation and refinement by a full-matrix least-squares procedure on F^2 (program *SHELXL-97*).[20a] An absorption correction was performed with the SADABS program (empirical absorption correction).[20b] Solvent molecules in the structure were highly disordered and impossible to refine by using conventional discrete-atom models. To resolve these issues, the contribution of the solvent electron density was removed by using the *SQUEEZE* routine in *PLATON*.[16] CCDC-831533 contains the supplementary crystallographic data for this paper. These data can be obtained free of charge from The Cambridge Crystallographic Data Centre via www.ccdc.ac.uk/data_request/cif.

Syntheses

[5,10,15,20-tetrakis(4-Carboxymethylphenyl)ethynylporphyrinato]zinc(II) (ZnTCPEP-Me_4): To a solution of 5,10,15,20-tetrakis(TIPS-ethynyl)porphyrin (**4**) (286 mg, 0.261 mmol) in a mixture of CH_2Cl_2 (10 mL) and THF (30 mL) was added TBAF (1.57 mL, 1 M in THF). After the mixture was stirred at room temperature for 1 h under ambient conditions, water (50 mL) was added. The solution was concentrated under reduced pressure, filtered, and washed with water. The obtained green solid was dried under vacuum to give the deprotected ethynylporphyrin. To a degassed solution of the deprotected ethynylporphyrin, methyl 4-iodobenzoate (547 mg, 2.09 mmol), and $AsPh_3$ (128 mg, 0.42 mmol) in a mixture of THF (100 mL) and Et_3N (10 mL) was added $Pd_2(dba)_3$ (15 mg, 0.0261 mmol). The mixture was stirred at 50 °C for 18 h. Upon cooling to room temperature, the resultant precipitate was filtered and washed with CH_2Cl_2. After drying under vacuum, ZnTCPEP-Me_4 was obtained as a purple solid (217 mg, 0.216 mmol, 82.6% yield). ^{1}H NMR (400 MHz, $CDCl_3$): δ = 9.25 (s, 8 H, β), 8.17 (d, J = 8.1 Hz, 8 H, Ph-*ortho*), 8.02 (d, J = 8.1 Hz, 8 H, Ph-*meta*), 4.05 (s, 6 H, -OCH_3) ppm. MS (MALDI-TOF$^+$): calcd. for $C_{60}H_{36}N_4O_8Zn$ [M$^+$] 1004.18; found 1004.11.

[5,10,15,20-tetrakis(4-Carboxyphenyl)ethynylporphyrinato]zinc(II) (ZnTCPEP-H_4): To a THF solution of ZnTCPEP-Me_4 (50 mg, 0.0497 mmol, 20 mL) was added aqueous NaOH solution (2 M, 0.25 mL, 0.500 mmol). The mixture was stirred at room temperature overnight. Then aqueous HCl solution (1 M, 20 mL) was added to neutralize the reaction mixture. The resultant precipitate was filtered and washed with H_2O. After drying under vacuum, the porphyrin complex ZnTCPEP-H_4 was obtained in quantitative yield as a greenish-purple solid. ^{1}H NMR (400 MHz, $CDCl_3$): δ = 9.37 (s, 8 H, β), 8.18 (dd, J = 20.4 and 8.18 Hz, 16 H, Ph-*ortho* and -*meta*) ppm. MS (MALDI-TOF$^+$): calcd. for $C_{56}H_{28}N_4O_8Zn$ [M$^+$] 948.12; found 947.59.

$[Zn_4(\mu_3\text{-}OH)_2(H_2O)_2(ZnTCPEP\text{-}H)_2(DABCO)_2]\cdot 2DMF\cdot 10.5H_2O$ ($Zn_4\cdot$ZnTCPEP$\cdot$DABCO): A mixture of $Zn(NO_3)\cdot 6H_2O$ (157 mg, 0.526 mmol), ZnTCPEP-H_4 (100 mg, 0.105 mmol), and DABCO (24 mg, 0.210 mmol) was dissolved in DMF/EtOH/H_2O (70:4:1) (75 mL) in a Teflon-lined stainless steel vessel. One drop of HCl (1 M) was added, and the solution was heated to 80 °C for 48 h. The resultant green block crystals were filtered, washed with DMF, and dried under vacuum to give $[Zn_4(\mu_3\text{-}OH)_2(H_2O)_2(ZnTCPEP\text{-}H)_2(DABCO)_2]\cdot 2DMF\cdot 10.5H_2O$ (146 mg, 99.8% yield). $C_{130}H_{115}N_{14}O_{32.5}Zn_6$ (2785.84): calcd. C 56.05, H 4.16, N 7.04; found C 55.92, H 3.80, N 7.20. IR: $\tilde{\nu}$ = 1654 (s), 1601 (s), 1538 (m), 1498 (w), 1386 (s) cm^{-1}. TG/DTA under atmospheric conditions: a weight loss of 15.7% was observed below 200 °C; calcd. 12.0% for 2DMF and 10.5H_2O.

Supporting Information (see footnote on the first page of this article): Selected bond lengths, TG/TDA plots, and powder XRD patterns for $Zn_4\cdot$ZnTCPEP$\cdot$DABCO.

---

[1] a) W. Mori, F. Inoue, K. Yoshida, H. Nakayama, S. Takamizawa, M. Kishita, *Chem. Lett.* **1997**, *26*, 1219–1220; b) H. Li, M. Eddaoudi, T. L. Groy, O. M. Yaghi, *J. Am. Chem. Soc.* **1998**, *120*, 8571–8572; c) K. Seki, S. Takamizawa, W. Mori, *Chem. Lett.* **2001**, *30*, 122–123; d) M. Kondo, T. Yoshitomi, K. Seki, H. Matsuzaka, S. Kitagawa, *Angew. Chem. Int. Ed. Engl.* **1997**, *36*, 1725–1727; e) L. J. Murray, M. Dincă, J. R. Long, *Chem. Soc. Rev.* **2009**, *38*, 1294–1314; f) J. L. C. Rowsell, O. M. Yaghi, *Angew. Chem. Int. Ed.* **2005**, *44*, 4670–4679; g) S. Kitagawa, R. Kitaura, S. Noro, *Angew. Chem. Int. Ed.* **2004**, *43*, 2334; h) D. Bradshaw, J. B. Claridge, E. J. Cussen, T. J. Prior, M. J. Rosseinsky, *Acc. Chem. Res.* **2005**, *38*, 273–282.

[2] a) T. Sato, W. Mori, C. N. Kato, T. Ohmura, T. Sato, K. Yokoyama, S. Takamizawa, S. Naito, *Chem. Lett.* **2003**, *32*, 854–855; b) T. Sato, W. Mori, C. N. Kato, E. Yanaoka, T. Kuribayashi, R. Ohtera, Y. Shiraishi, *J. Catal.* **2005**, *232*, 186–198; c) C. N. Kato, M. Ono, T. Hino, T. Ohmura, W. Mori, *Catal. Commun.* **2006**, *7*, 673–677; d) ; W. Mori, T. Sato, T. Ohmura, C. N. Kato, T. Takei, *J. Solid State Chem.* **2005**, *178*, 2555–2573; e) W. Mori, T. Sato, C. N. Kato, T. Takei, T. Ohmura, *Chem. Rec.* **2005**, *5*, 336–351; f) W. Mori, S. Takamizawa, C. N. Kato, T. Ohmura, T. Sato, *Microporous Mesoporous Mater.* **2004**, *73*, 31–46.

[3] a) D. Bradshaw, T. J. Prior, E. J. Cussen, J. B. Claridge, M. J. Rosseinsky, *J. Am. Chem. Soc.* **2004**, *126*, 6106–6114; b) E.-Y. Choi, K. Park, C.-M. Yang, H. Kim, J.-H. Son, S. W. Lee, Y. H. Lee, D. Min, Y.-U. Kwon, *Chem. Eur. J.* **2004**, *10*, 5535–5540; c) E. Y. Lee, S. Y. Jang, M. P. Suh, *J. Am. Chem. Soc.* **2005**, *127*, 6374–6381; d) M. Dincă, J. R. Long, *J. Am. Chem. Soc.* **2005**, *127*, 9376–9377; e) L. Pan, D. H. Olson, L. R. Ciemnolonski, R. Heddy, J. Li, *Angew. Chem. Int. Ed.* **2006**, *45*, 616–619; f) B. Chen, C. Liang, J. Yang, D. S. Contreras, Y. L. Clancy, E. B. Lobkovsky, O. M. Yaghi, S. Dai, *Angew. Chem. Int. Ed.* **2006**, *45*, 1390–1393; g) P. S. Bárcia, F. Zapata, J. A. C. Silva, A. E. Rodrigues, B. Chen, *J. Phys. Chem. B* **2007**, *111*, 6101–6103; h) S. Ma, D. Sun, X.-S. Wang, H.-C. Zhou, *Angew. Chem. Int. Ed.* **2007**, *46*, 2458–2462; i) Y.-S. Bae, K. L. Mulfort, H. Frost, P. Ryan, S. Punnathanam, L. J. Broadbelt, J. T. Hupp, R. Q. Snurr, *Langmuir* **2008**, *24*, 8592–8598; j) L. Bastin, P. S. Barcia, E. J. Hurtado, J. A. M. Silva, A. E. Rodrigues, B. Chen, *J. Phys. Chem. C* **2008**, *112*, 1575–1581; k) J.-R. Li, R. J. Kuppler, H.-C. Zhou, *Chem. Soc. Rev.* **2009**, *38*, 1477–1504.

[4] a) K. S. Min, M. P. Suh, *J. Am. Chem. Soc.* **2000**, *122*, 6834–6840; b) H. J. Choi, M. P. Suh, *Inorg. Chem.* **2003**, *42*, 1151–1157; c) M. Dincă, J. R. Long, *J. Am. Chem. Soc.* **2007**, *129*, 11172–11176; d) S. Yang, X. Lin, A. J. Blake, K. M. Thomas, P. Hubberstey, N. R. Champness, M. Schröder, *Chem. Commun.* **2008**, 6108–6110; e) F. Nouar, J. Eckert, J. F. Eubank, P. Forster, M. Eddaoudi, *J. Am. Chem. Soc.* **2009**, *131*, 2864–2870.

[5] a) M. Fujita, Y. J. Kwon, S. Washizu, K. Ogura, *J. Am. Chem. Soc.* **1994**, *116*, 1151–1152; b) K. Schlichte, T. Kratzke, S. Kaskel, *Microporous Mesoporous Mater.* **2004**, *73*, 81–88; c) C.-D. Wu, A. Hu, L. Zhang, W. Lin, *J. Am. Chem. Soc.* **2005**, *127*, 8940–8941; d) L. Alaerts, E. Séguin, H. Poelman, F. Thibault-Starzyk, P. A. Jacobs, D. E. D. Vos, *Chem. Eur. J.* **2006**, *12*, 7353–7363; e) S. Horike, M. Dincă, K. Tamaki, J. R. Long, *J. Am. Chem. Soc.* **2008**, *130*, 5854–5855; f) Y. K. Hwang, D.-Y. Hong, J.-S. Chang, S. H. Jhung, Y.-K. Seo, J. Kim, A. Vimont, M. Daturi, C. Serre, G. Férey, *Angew. Chem. Int. Ed.* **2008**, *47*, 4144–4148; g) A. Corma, M. Iglesias, F. X. Llabrés i Xamena, F. Sánchez, *Chem. Eur. J.* **2010**, *16*, 9789–9795; h) L. Ma, C. Abney, W. Lin, *Chem. Soc. Rev.* **2009**, *38*, 1248–1256; i) J. Lee, O. K. Farha, J. Roberts, K. A. Scheidt, S. T. Nguyen, J. T. Hupp, *Chem. Soc. Rev.* **2009**, *38*, 1450–1459.

[6] a) R. Kitaura, G. Onoyama, H. Sakamoto, R. Matsuda, S. Noro, S. Kitagawa, *Angew. Chem. Int. Ed.* **2004**, *43*, 2684–2687; b) M. Oh, C. A. Mirkin, *Angew. Chem. Int. Ed.* **2006**, *45*, 5492–5494; c) S.-H. Cho, B. Ma, S. T. Nguyen, J. T. Hupp, T. E. Albrecht-Schmitt, *Chem. Commun.* **2006**, 2563–2565; d) Y. M. Jeon, J. Heo, C. A. Mirkin, *J. Am. Chem. Soc.* **2007**, *129*, 7480–7481; e) S. Jung, M. Oh, *Angew. Chem. Int. Ed.* **2008**, *47*, 2049–2051; f) B. Chen, X. Zhao, A. Putkham, K. Hong, E. B. Lobkovsky, E. J. Hurtado, A. J. Fletcher, K. M. Thomas, *J. Am. Chem. Soc.* **2008**, *130*, 6411–6423; g) F. Song, C. Wang, J. M. Falkowski, L. Ma, W. Lin, *J. Am. Chem. Soc.* **2010**, *132*, 15390–15398.

[7] a) L. Carlucci, G. Ciani, D. M. Proserpio, F. Porta, *Angew. Chem. Int. Ed.* **2003**, *42*, 317–322; b) D. Hagrman, P. J. Hagrman, J. Zubieta, *Angew. Chem. Int. Ed.* **1999**, *38*, 3165–3168; c) M. E. Kosal, J.-H. Chou, S. R. Wilson, K. S. Suslick, *Nat. Mater.* **2002**, *1*, 118–121; d) D. W. Smithenry, S. R. Wilson, K. S. Suslick, *Inorg. Chem.* **2003**, *42*, 7719–7721; e) L. Pan, X. Huang, H.-L. N. Phan, T. J. Emge, J. Li, X. Wang, *Inorg. Chem.* **2004**, *43*, 6878–6880; f) T. Ohmura, A. Usuki, K. Fukumori, T. Ohta, M. Ito, K. Tatsumi, *Inorg. Chem.* **2006**, *45*, 7988–7990; g) A. M. Shultz, O. K. Farha, J. T. Hupp, S. T. Nguyen, *J. Am. Chem. Soc.* **2009**, *131*, 4204–4205; h) E.-Y. Choi, C. A. Wray, C. Hub, W. Choe, *CrystEngComm* **2009**, *11*, 553–555; i) R. Makiura, S. Motoyama, Y. Umemura, H. Yamanaka, O. Sakata, H. Kitagawa, *Nat. Mater.* **2010**, *9*, 565–571; j) K. S. Suslick, P. Bhyrappa, J.-H. Chou, M. E. Kosal, S. Nakagaki, D. W. Smithenry, S. R. Wilson, *Acc. Chem. Res.* **2005**, *38*, 283–291; k) O. K. Farha, A. M. Shultz, A. A. Sarjeant, S. T. Nguyen, J. T. Hupp, *J. Am. Chem. Soc.* **2011**, *133*, 5652–5655.

[8] O. K. Farha, A. M. Spokoyny, K. L. Mulfort, M. F. Hawthorne, C. A. Mirkin, J. T. Hupp, *J. Am. Chem. Soc.* **2007**, *129*, 12680–12681; Y.-S. Bae, O. K. Farha, A. M. Spokoyny, C. A. Mirkin, J. T. Hupp, R. Q. Snurr, *Chem. Commun.* **2008**, 4135–4137; A. M. Spokoyny, O. K. Farha, K. L. Mulfort, J. T. Hupp, C. A. Mirkin, *Inorg. Chim. Acta* **2010**, *364*, 266–271.

[9] J. W. Han, C. L. Hill, *J. Am. Chem. Soc.* **2007**, *129*, 15094–15095.

[10] K. M. Kadish, K. M. Smith, R. Guilard, *The Porphyrin Handbook*, Academic Press, San Diego, CA, **2000**.

[11] a) R. K. Kumar, S. Balasubramanian, I. Goldberg, *Inorg. Chem.* **1998**, *37*, 541–552; b) R. K. Kumar, I. Goldberg, *Angew. Chem. Int. Ed.* **1998**, *37*, 3027–3030; c) Y. Diskin-Posner, S. Dahal, I. Goldberg, *Chem. Commun.* **2000**, 585–586; d) Y. Diskin-Posner, G. K. Patra, I. Goldberg, *Eur. J. Inorg. Chem.* **2001**, 2515–2523; e) M. Shmilovits, Y. Diskin-Posner, M. Vinodu, I. Goldberg, *Cryst. Growth Des.* **2003**, *3*, 855–863; f) M. Shmilovits, M. Vinodu, I. Goldberg, *Cryst. Growth Des.* **2004**, *4*, 633–

638; g) M. Vinodu, I. Goldberg, *New J. Chem.* **2004**, *28*, 1250–1254; h) S. George, S. Lipstman, I. Goldberg, *Cryst. Growth Des.* **2006**, *6*, 2651–2654; i) S. Muniappan, S. Lipstman, S. George, I. Goldberg, *Inorg. Chem.* **2007**, *46*, 5544–5554; j) I. Goldberg, *Chem. Eur. J.* **2000**, *6*, 3863–3870; k) I. Goldberg, *CrystEngComm* **2008**, *10*, 637–645.

[12] a) B. Leibrock, O. Vostrowsky, A. Hirsch, *Eur. J. Org. Chem.* **2001**, 4401–4409; b) M. J. Plater, S. Aiken, G. Bourhill, *Tetrahedron* **2002**, *58*, 2415–2422.

[13] R. W. Wagner, T. E. Johnson, F. Li, J. S. Lindsey, *J. Org. Chem.* **1995**, *60*, 5266–5273.

[14] a) I. D. Brown, D. Altermatt, *Acta Crystallogr., Sect. B* **1985**, *41*, 244–247; b) I. D. Brown, R. D. Shannon, *Acta Crystallogr., Sect. A* **1973**, *29*, 266–282; c) I. D. Brown, *Acta Crystallogr., Sect. B* **1992**, *48*, 553–572; d) I. D. Brown, *J. Appl. Crystallogr.* **1996**, *29*, 479–480.

[15] D. Sun, Y. Ke, T. M. Mattox, S. Parkin, H.-C. Zhou, *Inorg. Chem.* **2006**, *45*, 7566–7568.

[16] A. L. Spek, *J. Appl. Crystallogr.* **2003**, *36*, 7–13.

[17] a) E.-Y. Choi, P. M. Barron, R. W. Novotny, H.-T. Son, C. Hu, W. Choe, *Inorg. Chem.* **2009**, *48*, 426–428; b) P. M. Barron, H.-T. Son, C. Hu, W. Choe, *Cryst. Growth Des.* **2009**, *9*, 1960–1965; c) H. Chung, P. M. Barron, R. W. Novotny, H.-T. Son, C. Hu, W. Choe, *Cryst. Growth Des.* **2009**, *9*, 3327–3332; d) J. M. Verduzco, H. Chung, C. Hu, W. Choe, *Inorg. Chem.* **2009**, *48*, 9060–9062.

[18] A. Saito, H. C. Foley, *AIChE J.* **1991**, *37*, 429–436.

[19] M. C. Burla, R. Caliandro, M. Camalli, B. Carrozzini, G. L. Cascarano, L. De Caro, C. Giacovazzo, G. Polidori, R. Spagna, *J. Appl. Crystallogr.* **2005**, *38*, 381–388.

[20] a) G. M. Sheldrick, *SHELXL-97 Program for Crystal Structure Refinement*, University of Göttingen, Germany, **1997**; b) G. M. Sheldrick, *SADABS*, University of Göttingen, Germany, **1996**.

Received: June 29, 2011